Preprint typeset using LaTeX style emulateapj v. 12/14/05



# THE EVOLVING FAINT-END OF THE LUMINOSITY FUNCTION

S. Khochfar[1], J. Silk[1], R. A. Windhorst[2], R. E. Ryan Jr.[3]
[1] Department of Physics, Denys Wilkinson Bldg., University of Oxford, Keble Road, Oxford, OX1 3RH, UK
[2] School of Earth and Space Exploration, Arizona State University, Tempe, AZ, 85287
[3] Department of Physics, Arizona State University, Tempe, AZ, 85287

## ABSTRACT

We investigate the evolution of the faint-end slope of the luminosity function, $\alpha$, using semi-analytical modeling of galaxy formation. In agreement with observations, we find that the slope can be fitted well by $\alpha(z) = a + bz$, with $a = -1.13$ and $b = -0.1$. The main driver for the evolution in $\alpha$ is the evolution in the underlying dark matter mass function. Sub-$L_*$ galaxies reside in dark matter halos that occupy a different part of the mass function. At high redshifts, this part of the mass function is steeper than at low redshifts, and hence $\alpha$ is steeper. Supernova feedback in general causes the same relative flattening with respect to the dark matter mass function. The faint-end slope at low redshifts is dominated by field galaxies and at high redshifts by cluster galaxies. The evolution of $\alpha(z)$ in each of these environments is different, with field galaxies having a slope $b = -0.14$ and cluster galaxies $b = -0.05$. The transition from cluster-dominated to field-dominated faint-end slope occurs roughly at a redshift $z_* \simeq 2$, and suggests that a single linear fit to the overall evolution of $\alpha(z)$ might not be appropriate. Furthermore, this result indicates that tidal disruption of dwarf galaxies in clusters cannot play a significant role in explaining the evolution of $\alpha(z)$ at $z < z_*$. In addition we find that different star-formation efficiencies $a_*$ in the Schmidt-Kennicutt-law and supernovae-feedback efficiencies $\epsilon$ generally do not strongly influence the evolution of $\alpha(z)$.

*Subject headings:* galaxies: evolution – methods: numerical

## 1. INTRODUCTION

The galaxy luminosity function (LF) is one of the cornerstones in our understanding of galaxy formation and evolution. Since the introduction of a fitting function for its shape by Schechter (1976), the origin of the form of the LF function has been a powerful constraint on model building (e.g., Benson et al. 2003; Samui et al. 2007). While recent work has focused somewhat on the luminous end, its evolution with redshift (Brown et al. 2007) and the role of dry mergers (Khochfar & Burkert 2003; Naab et al. 2006), the faint-end provides additional important clues on galaxy formation. Systematic studies of the faint-end slope in the local universe reveal differences between high and low density environments (Trentham 1998), as well as for galaxy samples split by morphologies (e.g. Marzke et al. 1994). The underlying physical processes that shape the faint-end of the LF are generally associated with feedback from supernovae that is effective in heating gas and driving winds in shallow gravitational potentials (Dekel & Silk 1986). Although the implementation of supernova feedback in galaxy formation models has been extensively investigated (e.g. Benson et al. 2003) for the local galaxy LF, its impact on the redshift evolution on the faint-end has not been as well studied. The recent wealth of LF measured to very faint magnitudes in the rest-frame B-band (e.g. Blanton et al. 2003; Wolf et al. 2003; Marchesini et al. 2007; Ryan et al. 2007) and the rest-frame FUV (e.g. Yan & Windhorst 2004a; Wyder et al. 2005; Bouwens et al. 2006) allows us to test models with high accuracy.

The purpose of this letter is to investigate the underlying driving mechanism for the redshift evolution of the faint-end slope. Furthermore, we investigate the impact of supernova feedback on the rate of star-formation by varying the relevant efficiency parameters.

## 2. MODEL

In the following we briefly outline our basic modelling approach and refer the reader for more details to Khochfar & Burkert (2005), Khochfar & Silk (2006) and reference therein. We generate merger trees for dark matter halos using a Monte-Carlo approach based on the extended Press-Schechter formalism (Somerville & Kolatt 1999). As we aim to model the faint-end of the LF to high redshifts, we need to make sure that the mass resolution in our simulations is sufficient. We generate merger trees from dark matter mass functions between $z = 0$ and $z = 6$, and find that resolving each individual merger tree down to a mass resolution of $M_{\rm min} = 5 \times 10^9$ $M_\odot$ and $M_{\rm min} = 10^8$ $M_\odot$ at $z \leq 3$ and $z \geq 4$, respectively, gives robust results. Once a tree reaches $M_{min}$, we start moving the tree forward in time including physical processes associated with the baryons within each dark matter halo that include gas cooling, star-formation, supernova feedback, reionization and merging of galaxies on a dynamical friction time-scale. As the focus of this letter is on the faint-end of the luminosity function, we will omit including prescriptions for AGN-feedback (e.g. Bower et al. 2006) or environmental effects (Khochfar & Ostriker 2007) that mainly influence the bright-end of the luminosity function.

The largest impact on the slope at the faint-end comes from star-formation and associated supernova feedback (Dekel & Silk 1986). Faint galaxies generally occupy small dark matter halos with shallow potential wells, that allow effective reheating of cold gas in the ISM by feedback from supernovae. We model star-formation in galaxies using a parametrisation of the

global Schmidt-Kennicutt-law (Kennicutt 1998) according to which $\dot{M}_* = a_* M_{cold}/t_{dyn}$, where $a_*$ is a free parameter that is indicative of the efficiency of star-formation, $M_{cold}$ is the mass in cold gas in the galactic disk, and $t_{dyn}$ is the dynamical time-scale of the galaxy. Following the arguments by Dekel & Silk (1986), we model the amount of cold gas reheated by feedback from supernovae with $\dot{M}_{SN} = 4\epsilon \dot{M}_* \eta_{SN} E_{SN}/3V_{max}^2$, with $\epsilon$ as a free parameter that controls the feedback efficiency, $\eta_{SN}$ the number of supernovae per solar mass of stars formed, $E_{SN} = 10^{51}$ erg is the energy released by each supernova, and $V_{max}$ is the maximum circular velocity of the dark matter halo in which the galaxy resides.

For each individual galaxy in our simulation, we store the star-formation history and generate its $B-$band and FUV rest-frame luminosity function at various redshifts using the stellar population models of Bruzual & Charlot (2003). The faint-end of the luminosity function is then fitted by a simple power law with slope $\alpha$ as defined in Schechter (1976). We fit the faint-end LF at each redshift with a power law spanning a range of four magnitudes at z $\leq$ 3 and at least two magnitudes at $z > 3$, starting at the lowest magnitude $L_{min}$ that is unaffected by the mass resolution of the simulation. We choose this approach over fitting the whole LF with a Schechter-fit, because we are missing physical effects (see below) in our model that are responsible for shaping the bright-end and the knee of the LF. In addition, we increase the number of magnitude bins and make sure that the fitted values for $\alpha$ are unaffected by the bin-size. Fig.1 shows the luminosity function at magnitudes larger than the corresponding minimum magnitude for $L_{min}$. In this study, we simulate a volume of $10^6$ Mpc$^3$, which allows us to calculate $\alpha$ robustly up to a redshift $z \simeq 6$.

Throughout this paper, we use the following set of cosmological parameters based on the three year Wilkinson Microwave Anisotropy Probe data (Spergel et al. 2007): $\Omega_0 = 0.27$, $\Omega_\Lambda = 0.73$, $\Omega_b/\Omega_0 = 0.17$, $\sigma_8 = 0.77$ and $h = 0.71$.

## 3. RESULTS

There is significant evidence that the faint-end slope of the galaxy luminosity function shows a measurable dependence on redshift, which can be fitted by a linear law of the form $\alpha(z) = a + bz$, with $a$ between $-1.12$ and $-1.17$, and $b$ between $-0.12$ and $-0.11$ (for recent observations, see Sawicki & Thompson 2006; Marchesini et al. 2007; Ryan et al. 2007). Within the hierarchical structure formation paradigm, one naturally expects such behaviour, considering that the slope of the dark matter mass function below $M_{DM,*}$ is $\alpha_{DM} \sim 2$ and that the objects that form in these halos continue to grow by continued star-formation and mergers with each other (Khochfar & Burkert 2001), hence flattening the slope. Fig. 1 shows the predicted model luminosity function at various redshifts in the rest-frame $B$ and $UV$. The simulated and observed luminosity functions are in fair agreement at the faint-end. The luminous end however, shows deviations at low redshift which are due to missing feedback sources in massive galaxies such as AGN or to environmental effects. In Fig. 2, we show the predicted evolution of $\alpha(z)$ for our best-fit local model. The free parameters $a_*$ and $\epsilon$ in this model are chosen to give the best fit to various local observations (see Khochfar & Silk 2006). For consistency with the majority of observations, we calculate the faint-end slope for the rest-frame FUV at $z \geq 4$ and at lower redshifts for the rest-frame $B$-band. We indeed find an evolution in $\alpha$ with redshift that is in fair agreement with the observed evolution.

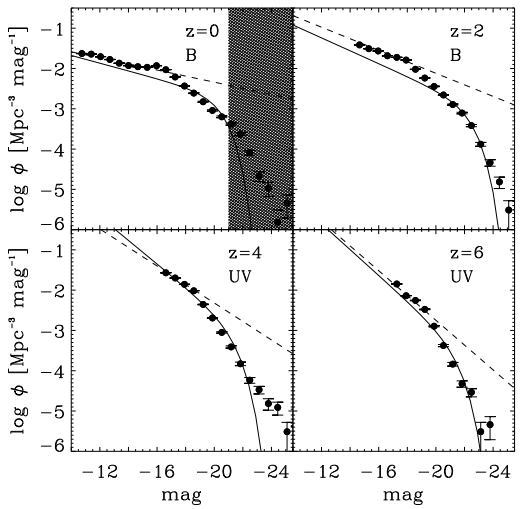


FIG. 1.— Comparison between model LFs with $\epsilon = 0.6$ and $\alpha = 0.02$ (symbols), and Schechter fits to various observations of the LF at different redshifts (solid lines). The dashed lines show our power law fits to the faint-end of the LF. Top left panel: Rest-frame $B-$band LF from Norberg et al. (2002), where we assumed that $B = b_j + 0.12$ mag. The shaded area indicates the region of the LF that is not well matched due to missing feedback effects. Top right panel: Rest-frame $B-$band LF from (Marchesini et al. 2007). Bottom left: UV-LF from Bouwens et al. (2007). Bottom right: UV-LF from Yan & Windhorst (2004b). Following Bouwens et al. (2006), we assume an average dust correction 0.4 mag at $z \geq 4$.

The immediate question that arises is, what influences and is the main driver for the evolution in $\alpha$? Generally, supernova feedback is considered the dominant mechanism in shaping the faint-end of the luminosity function (Dekel & Silk 1986; Benson et al. 2003). The shaded region in Fig. 2 shows the range of linear fits to $\alpha(z)$ that we find by varying the star-formation efficiency between $a_* = 0.02-0.1$ and the supernovae feedback efficiency between $\epsilon = 0.2 - 0.6$. We infer only a very modest change in $\alpha(z)$ for reasonable choices of feedback efficiencies, and therefore conclude that another process must be responsible for the observed evolution in $\alpha(z)$.

The mass function of dark matter halos is known to show a strong evolution with redshift (e.g. Press & Schechter 1974). The galaxies contributing to the luminosity function around $L_*$ are mostly central galaxies in their dark matter halos, i.e. the most luminous galaxy within the halo (e.g. Khochfar & Ostriker 2007). It is therefore not unreasonable to assume a connection between the evolution of $\alpha(z)$ and that of the dark matter mass function. When considering the luminosity of central galaxies residing in dark matter halos of the same mass at different redshifts, we find that at early times, central galaxies are up to three magnitudes brighter than their counterparts in low redshift halos. This is even the case for halos hosting sub-$L_*$ galaxies. Similar results have been reported by Kobayashi et al. (2007), who showed that dwarf galaxies at early times are not affected by supernova feedback in their simula-

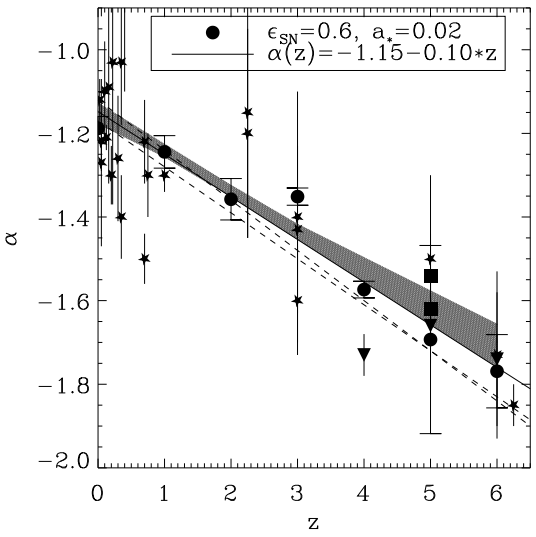


FIG. 2.— The slope $\alpha$ at different redshifts as predicted by the best fit local model with $a_* = 0.02$, $\epsilon = 0.6$. Filled symbols show results from the simulation and the solid line is the best fit to the simulation data. Errorbars indicate 1-$\sigma$ errors. The dashed lines show the fit to the compiled data in Ryan et al. (2007). The shaded region shows the range of linear fits to $\alpha(z)$ that we find when varying the star-formation and supernovae feedback efficiencies as discussed in the text. Stars are the compilation from Ryan et al. (2007). The filled squares and triangles show recent results from Oesch et al. (2007) and Bouwens et al. (2007), respectively.

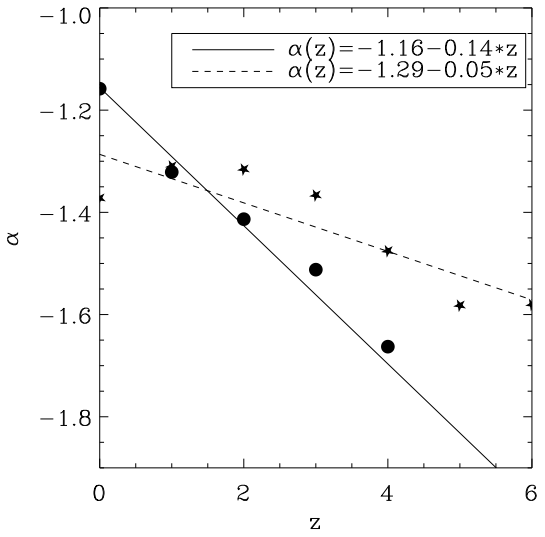


FIG. 3.— The slope $\alpha$ at different redshifts as predicted by the best fit local model. Filled circles show results for typcal field environments and filled stars show the results for cluster environments, as defined by their present day dark halo mass. The solid and dashed line are the fits to the modeled evolution in the field and cluster, respectively. Here we define cluster environments by present-day dark matter halos above $10^{14}$ $M_\odot$ and field environments, by halos with masses below $10^{12}$ $M_\odot$.

tions because cooling times are very short in these halos and the energy injected by the supernovae is rapidly dissipated away. The slope in the region of dark matter halos that host sub-$L_*$ galaxies is steeper at high redshift, and consequently so is $\alpha$. The same is true for other choices of $a_*$ and $\epsilon$, thereby explaining why we do not find any strong dependence of $\alpha(z)$ on these parameters. It should be noted however, that modelling these parameters with a strong redshift dependency will be able to enhance or weaken the evolution of $\alpha$

We continue analyzing the evolution in $\alpha(z)$ by distinguishing between cluster and field galaxies and their relaxation to the overall luminosity function at the faint-end. In Fig. 3, we present $\alpha(z)$ for progenitor galaxies of present-day cluster and field galaxies from our simulations. Here we define cluster environments by present-day dark matter halos above $10^{14}$ $M_\odot$, and field environments by halos with masses below $10^{12}$ $M_\odot$. In field environments $\alpha$ is steeper and evolves more strongly than in cluster environments. At early times, the first galaxies to appear are most likely in high$-\sigma$ fluctuations, which will result in present-day galaxy clusters. Consequently, the faint-end luminosity function at high redshifts will be dominated by present-day cluster members, and the faint-end-slope of the overall galaxy population at high redshifts is flatter than that for the field luminosity function alone at the same redshift. When considering the relative weight of field galaxies to the overall galaxy population at the faint-end, one can estimate the redshift at which the transition from cluster-driven to field-driven evolution in $\alpha$ occurs. We find that this transition roughly occurs at $z_* \simeq 2$ with a slight dependency on the definition of environment.

## 4. DISCUSSION AND CONCLUSIONS

In this Letter, we presented predictions for the redshift evolution of the faint-end slope of the luminosity function within the ΛCDM-scenario. In general, we find the same trend as in the recent observations i.e., a steepening faint-end slope $\alpha$ with redshift, which can be well-fitted by a simple linear fit $\alpha(z) = a + bz$ where the observations find $a \simeq 1.17$ and $b \simeq -0.11$ (Ryan et al. 2007). Our simulations predict $a \simeq 1.13$ and $b \simeq -0.1$, in good agreement with the observations considering the large uncertainties, especially at high redshifts.

Our simulations confirm previous results that the flattening of the faint-end slope $\alpha$ with respect to the slope in the dark matter mass function can be well explained by supernova feedback. However we additionally show that $\alpha$ is steeper at higher redshifts mainly, due to the dark matter mass function being steeper for the range of halo masses that host sub-$L_*$ galaxies, suggesting that the evolution of $\alpha$ traces closely that of the underlying dark matter mass function.

The contribution of the progenitor population of present-day field and cluster galaxies plays a significant role in shaping the evolution of $\alpha$ . For field galaxies, the evolution of $\alpha(z)$ is stronger, with $b = -0.14$ and $a = -1.16$ than for cluster galaxies. In our simulations, we find that at redshifts $z \geq 2$, the faint-end is dominated by galaxies ending up in present-day clusters. This transition redshift is dependent on the value of $\sigma_8$, which normalizes the power spectrum and regulates the redshift at which structures of a given mass typically form. Additionally, the slope of the fluctuation spectrum at small scales will influence $z_*$. Precise high redshift measurements of the contributions of these two populations to the faint-end of the luminosity function in future surveys with e.g. the HST WFC3 will help to pin down $z_*$. One potential problem for future surveys will be a possible bias towards cluster galaxies as they might experience induced star-formation (Marcillac et al. 2007), increas-

ing their surface brightness and making them more easily detectable. This effect will shift $z_*$ to higher redshifts and needs to be taken into account carefully. Observational selection effects will affect the observed faint-end LF-slope in Fig. 2. Some observational selection effects (i.e. catalogue incompleteness and natural confusion, Windhorst et al. 2007) can make the observed faint-end slope flatter than the true one, while others (e.g., SB-dimming) could make the observed slope somewhat steeper than the true one, depending on the exact intrinsic object size distribution. A number of groups correct for incompleteness either through MC-simulations (e.g. Yan & Windhorst 2004b) or through cloning techniques (e.g. Bouwens et al. 2006), and find similar faint-end slopes when following different procedures. When judging the data, however, one must keep these observational biases in mind. Ultimately, these issues can only be resolved with deeper JWST data to AB=31-32 mag.

Tidal disruption of dwarf galaxies in clusters as seen in high resolution simulations (Tormen et al. 1998) can in principle change the slope $\alpha$. Our results, however, suggest that at a transition redshift of $z_* = 2$, the evolution of $\alpha$ changes from being dominated by cluster galaxies to being dominated by field galaxies. It is therefore not likely that a large amount of the evolution in $\alpha$ at $z < z_*$ is driven by tidal disruption of faint galaxies. An additional implication from the transition at $z_*$ is that the evolution of $\alpha(z)$ is better fit by a linear function with a break at $z_*$.

The flattening of the slope $\alpha$ with respect to the underlying dark matter slope suggests the interesting possibility of estimating the time-scale over which supernovae operate. Assuming that the first Pop II stars were formed sometime before reionization (Yan & Windhorst 2004b), and that supernovae type Ia originate roughly $\leq 1-2$ Gyr after the bulk of the first Pop II star-formation, one would expect an increase in energy injection into the interstellar medium at a redshift corresponding to this time lag. This additional energy input will hinder star-formation and contribute to a further increase in the mass-to-light ratio of galaxies and hence to an even stronger flattening of the slope $\alpha$. It will be crucial to have robust measurements of $\alpha$ over a wide range of redshifts to probe the onset of the first significant feedback contribution from type Ia supernovae. Furthermore, probing the faint-end slope at redshifts $z > 6$, before the significant onset of type II supernovae will allow us to measure the underlying dark matter slope very accurately.

Our approach has certain shortcomings. The model presented here did not include any time delay prescriptions for the various SN types, but instead assumed instantaneous feedback. More detailed modeling of the time delays and its influence on the faint-end slope will be presented elsewhere (in preparation). Our treatment of supernovae feedback is very simplistic, and more detailed hydrodynamical simulations including a multi-phase medium will show if this general trend which we report can be recovered. First generations of such simulations indeed show that SN type II that are generated in dense star clusters explode into bubbles of hot gas and are therefore less efficient at feedback into the ISM (Mac Low & Ferrara 1999) compared to SN type Ia, which go off at random places in the galaxy and, can have more effect on the early ISM.

We would like to thank Seth Cohen, Evan Scannapieco and Richard Bouwens for helpful discussions and the anonymous referee for his useful comments. This work was supported by HST grants HST-GO-10530.07 (to RAW) and HST-AR-10974.01 (to RER) from STScI, which is operated by AURA for NASA under contract NAS 5-26555, and by NASA JWST grant NAG 5-12460 (to RAW).

REFERENCES

Benson, A. J., Bower, R. G., Frenk, C. S., Lacey, C. G., Baugh, C. M., & Cole, S. 2003, ApJ, 599, 38
Blanton, M. R., et al. 2003, ApJ, 592, 819
Bouwens, R. J., Illingworth, G. D., Blakeslee, J. P., & Franx, M. 2006, ApJ, 653, 53
Bouwens, R. J., Illingworth, G. D., Franx, M., & Ford, H. 2007, ArXiv e-prints, 707, arXiv:0707.2080
Bower, R. G., Benson, A. J., Malbon, R., Helly, J. C., Frenk, C. S., Baugh, C. M., Cole, S., & Lacey, C. G. 2006, MNRAS, 370, 645
Brown, M. J. I., Dey, A., Jannuzi, B. T., Brand, K., Benson, A. J., Brodwin, M., Croton, D. J., & Eisenhardt, P. R. 2007, ApJ, 654, 858
Bruzual, G., & Charlot, S. 2003, MNRAS, 344, 1000
Cole, S., et al. 2001, MNRAS, 326, 255
Dekel, A., & Silk, J. 1986, ApJ, 303, 39
Huang, J.-S., Glazebrook, K., Cowie, L. L., & Tinney, C. 2003, ApJ, 584, 203
Jenkins, A., Frenk, C. S., White, S. D. M., Colberg, J. M., Cole, S., Evrard, A. E., Couchman, H. M. P., & Yoshida2007, N. 2001, MNRAS, 321, 372
Kennicutt, R. C., Jr. 1998, ApJ, 498, 541
Khochfar, S., & Burkert, A. 2001, ApJ, 561, 517
Khochfar, S., & Burkert, A. 2003, ApJ, 597, L117
Khochfar, S., & Burkert, A. 2005, MNRAS, 359, 1379
Khochfar, S., & Silk, J. 2006, MNRAS, 370, 902
Khochfar, S., & Ostriker, J. P. 2007, ArXiv e-prints, 704, arXiv:0704.2418
Kobayashi, C., Springel, V., & White, S. D. M. 2007, MNRAS, 376, 1465
Marchesini, D., et al. 2007, ApJ, 656, 42
Marcillac, D., Rigby, J. R., Rieke, G. H., & Kelly, D. M. 2007, ApJ, 654, 825
Marzke, R. O., Geller, M. J., Huchra, J. P., & Corwin, H. G., Jr. 1994, AJ, 108, 437
Mac Low, M.-M., & Ferrara, A. 1999, ApJ, 513, 142
Naab, T., Khochfar, S., & Burkert, A. 2006, ApJ, 636, L81
Norberg, P., et al. 2002, MNRAS, 336, 907
Oesch, P. A., et al. 2007, ArXiv e-prints, 706, arXiv:0706.2653
Press, W. H., & Schechter, P. 1974, ApJ, 187, 425
Ryan, R. E., Jr., et al. 2007, ArXiv Astrophysics e-prints, arXiv:astro-ph/0703743
Schechter, P. 1976, ApJ, 203, 297
Sawicki, M., & Thompson, D. 2006, ApJ, 648, 299
Samui, S., Srianand, R., & Subramanian, K. 2007, MNRAS, 377, 285
Schiminovich, D., et al. 2005, ApJ, 619, L47
Somerville, R. S., & Kolatt, T. S. 1999, MNRAS, 305, 1
Spergel, D. N., et al. 2007, ApJS, 170, 377
Tormen, G., Diaferio, A., & Syer, D. 1998, MNRAS, 299, 728
Trentham, N. 1998, MNRAS, 294, 193
Trentham, N., Sampson, L., & Banerji, M. 2005, MNRAS, 357, 783
Wolf, C., Wisotzki, L., Borch, A., Dye, S., Kleinheinrich, M., & Meisenheimer, K. 2003, A&A, 408, 499
Windhorst, R. A., Hathi, N. P., Cohen, S. H., Jansen, R. A., Kawata, D., Driver, S. P., & Gibson, B. 2007, Advances in Space Research, Vol. 9163, p.001–013, in press (astro-ph/0703171)
Wyder, T. K., et al. 2005, ApJ, 619, L15
Yan, H., & Windhorst, R. A. 2004a, ApJ, 612, L93
Yan, H., & Windhorst, R. A. 2004b, ApJ, 600, L1